Marquette University
e-Publications@Marquette

Civil and Environmental Engineering Faculty Research and Publications

Civil and Environmental Engineering, Department of

1-1-2014

Timoshenko Beam Model for Lateral Vibration of Liquid-Phase Microcantilever-Based Sensors

Joshua A. Schultz
Marquette University

Stephen M. Heinrich
Marquette University, stephen.heinrich@marquette.edu

Fabien Josse
Marquette University, fabien.josse@marquette.edu

Isabelle Dufour
Université de Bordeaux

Nicholas J. Nigro
Marquette University, nicholas.nigro@marquette.edu

See next page for additional authors

Authors

Joshua A. Schultz, Stephen M. Heinrich, Fabien Josse, Isabelle Dufour, Nicholas J. Nigro, Luke A. Beardslee, and Oliver Brand

Timoshenko Beam Model for Lateral Vibration of Liquid-Phase Microcantilever-Based Sensors

Joshua A. Schultz

Civil and Environmental Engineering, Marquette University
Milwaukee, WI

Stephen M. Heinrich

Civil and Environmental Engineering, Marquette University
Milwaukee, WI

Fabien Josser

Electrical and Computer Engineering, Marquette University
Milwaukee, WI

Isabelle Dufour

Université de Bordeaux, CNRS, IMS Laboratory
Talence, France

Nicholas J. Nigro

Mechanical Engineering, Marquette University
Milwaukee, WI

Luke A. Beardslee

School of Electrical and Computer Engineering, Georgia Institute of Technology
Atlanta, GA

Oliver Brand

School of Electrical and Computer Engineering, Georgia Institute of Technology
Atlanta, GA

Abstract:

Dynamic-mode microcantilever-based devices are potentially well suited to biological and chemical sensing applications. However, when these applications involve liquid-phase detection, fluid-induced dissipative forces can significantly impair device performance. Recent experimental and analytical research has shown that higher in-fluid quality factors (Q) are achieved by exciting microcantilevers in the lateral flexural mode. However, experimental results show that, for microcantilevers having larger width-to-length ratios, the behaviors predicted by current analytical models differ from measurements. To more accurately model microcantilever resonant behavior in viscous fluids and to improve understanding of lateral-mode sensor performance, a new analytical model is developed, incorporating both viscous fluid effects and "Timoshenko beam" effects (shear deformation and rotatory inertia). Beam response is examined for two harmonic load types that simulate current actuation methods: tip force and support rotation. Results are expressed in terms of total beam displacement and beam displacement due solely to bending deformation, which correspond to current detection methods used with microcantilever-based devices (optical and piezoresistive detection, respectively). The influences of the shear, rotatory inertia, and fluid parameters, as well as the load/detection scheme, are investigated. Results indicate that load/detection type can impact the measured resonant characteristics and, thus, sensor performance, especially at larger values of fluid resistance.

Keywords: Timoshenko beam, microcantilever-based sensors, quality factor, resonant frequency, fluid-solid interaction.

INTRODUCTION

Chemical and biological sensing is a rapidly developing field, resulting in an ever-increasing presence of micro/nanoelectromechanical systems (MEMS/NEMS) in a variety of diagnostic, monitoring, and security applications. However, many of these applications require liquid-phase sensing, which poses significant challenges for dynamic-mode sensors due to the drastic reductions in resonant frequency (f_{res}) and quality factor (Q) that occur due to the liquid. To meet such challenges, recent research has explored the use of alternative vibrational modes of micro/nanocantilever devices in lieu of the fundamental transverse, or out-of-plane, flexural mode. In particular, advantages associated with the use of lateral (inplane) flexural modes have been pursued [1-9]. These studies were motivated by the goal of reducing the detrimental effects of fluid damping and fluid inertia, thus providing higher resonant frequencies, f_{res}, and quality factors, Q, the latter corresponding to sharper resonance peaks. Such improvements in the resonant characteristics of the device translate into corresponding enhancements in sensor sensitivity and limit of detection, especially for liquid-phase detection [6, 10].

Some of the previously mentioned studies on the use of the in-plane flexural mode demonstrated both theoretically [3, 4, 8] and experimentally [5, 7] that the improvements in the in-liquid resonant characteristics will be most pronounced in microcantilevers that are relatively short and wide. However, the conclusions in the theoretical studies were based on EulerBernoulli beam models whose accuracy is known to deteriorate for short, wide beams deforming in the lateral mode due to the neglected "Timoshenko beam effects" of shear deformation and rotatory inertia. As these are exactly the geometries that show the most promise for lateral-mode, liquid-phase sensing, a strong motivation exists to generalize the previous Euler- Bernoulli modeling efforts to the realm of Timoshenko beam theory. Thus, the aim of the present paper is to present a Timoshenko beam model for a laterally vibrating microcantilever in the presence of a viscous fluid and to examine the theoretical beam response for two types of harmonic excitation that simulate current actuation methods: tip force and support rotation. Results will be expressed in terms of total beam

displacement and beam displacement due solely to bending deformation, which correspond to current detection methods used with microcantilever-based devices (optical and piezoresistive detection, respectively). The influences of the shear, rotatory inertia, and fluid parameters, as well as the actuation/detection scheme, will be investigated.

PROBLEM STATEMENT

Consider a microcantilever beam immersed in a viscous fluid which experiences an in-plane flexural vibration. The effects of shear deformation and rotatory inertia in the beam ("Timoshenko beam effects") are to be included, as are the inertial and damping effects of the surrounding fluid. The geometric parameters (L, b, h) and material density and elastic moduli (ρ_b, E, G) of the cantilever are indicated in Fig. 1, as are the fluid's density and viscosity (ρ_f, η). The loading parameters for the two load cases to be considered are shown in Fig. 2.

Load Case I involves a harmonically varying imposed rotation at the supported end, with amplitude θ_0 and frequency ω. In Load Case II the beam is excited by a harmonically varying tip force of amplitude F_0 and frequency ω. These load cases are considered because they represent two of the more common actuation methods used in microcantilever-based sensing applications. Load Case I simulates an electrothermal excitation scheme [5], involving thermally induced longitudinal thermal strains at the extreme fibers near the support. Such a loading may be represented kinematically as an imposed
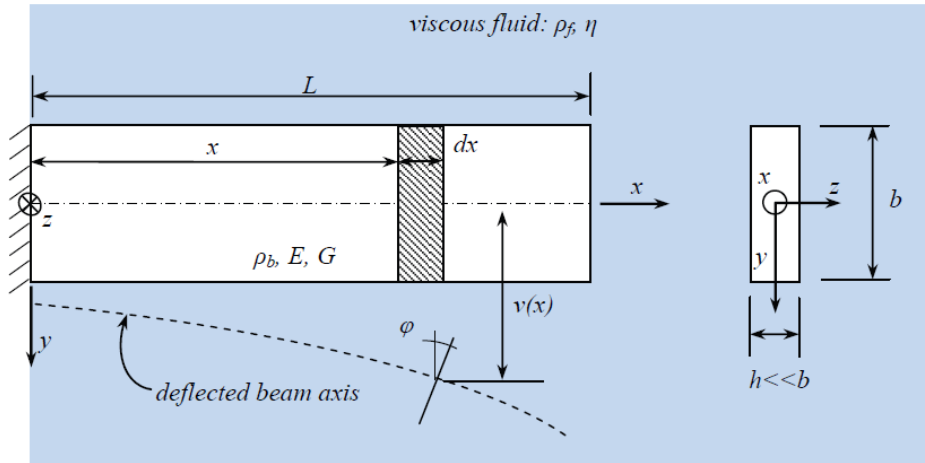
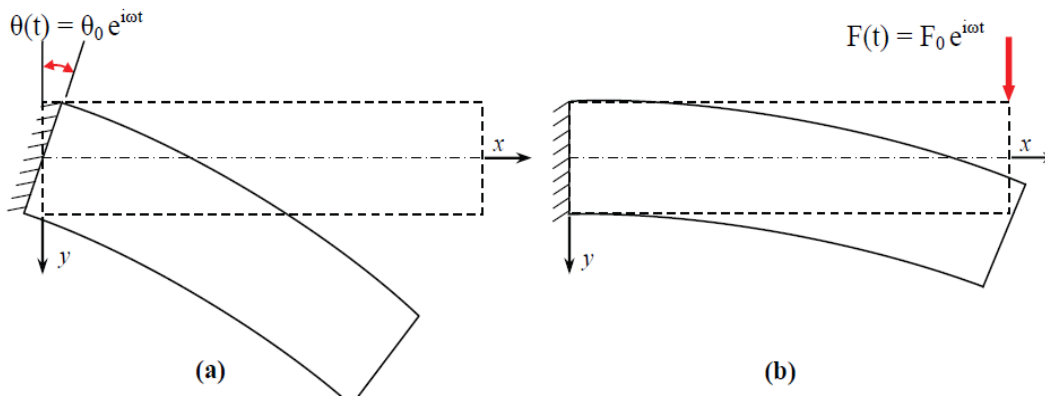**Fig. 1** Definitions of Geometric and Material Parameters

Fig. 2 (a) Load Case I – Imposed Harmonic Support Rotation; (b) Load Case II – Imposed Harmonic Tip Force

harmonic rotation at the support [4]. Load Case II is chosen because a tip force loading may be induced via electromagnetic actuation methods, commonly used in dynamic-mode sensing applications. For each load case our focus will be on examining two particular response histories: the total displacement at the beam tip and the bending-deformation displacement at the beam tip, the latter being that portion of the total tip displacement which is due to bending deformation *only*. The total tip displacement is the relevant output signal if microcantilever response is monitored by optical (laser) methods, while the bending-deformation displacement of the tip as predicted by the model provides an indirect measure of the beam's bending strain,

i.e., it will correspond to the output signal generated by piezoresistive elements that may be used to monitor beam response [5]. (This correlation is valid in the vicinity of a resonant peak since the vibrational shape due to bending deformation is relatively constant.) Of particular interest are the resonant frequency, f_{res}, and the quality factor, Q, associated with viscous losses in the surrounding fluid. These may be correlated to sensor performance metrics, i.e., mass and chemical sensitivities and limit of detection.

THEORETICAL MODEL

To derive the Timoshenko beam model the following assumptions are made: (1) the beam is homogeneous, linear elastic, and isotropic; (2) deformations are small; (3) the beam is attached to a rigid support at one end (see left end in Figs. 1 and 2); (4) the cross section is relatively thin ($h<<b$) so that the fluid resistance on the smaller faces is negligible; (5) the shear stress exerted by the fluid on the beam is modeled by local application of the solution of Stokes's second problem for harmonic, inplane oscillations of an infinite rigid surface in contact with a viscous fluid [11]; (6) the viscous energy dissipation in the fluid is the dominant loss mechanism. In tandem assumptions 4 and 5 shall be referred to the assumption of "Stokes fluid resistance," as was the case in earlier Bernoulli-Euler models [3, 4].

The foregoing assumptions (and the consideration of loads as specified in Load Cases I and II) result in the following governing equations for the lateral vibration of a harmonically excited Timoshenko beam in a viscous fluid providing Stokes resistance:

$$\frac{\partial^2 \overline{v}}{\partial \xi^2} - \frac{\partial \varphi}{\partial \xi} - s^2 \lambda^3 (\lambda + \zeta) \frac{\partial^2 \overline{v}}{\partial \tau^2} - s^2 \lambda^3 \zeta \frac{\partial \overline{v}}{\partial \tau} = 0 ,$$

(1a)

$$s^2 \frac{\partial^2 \varphi}{\partial \xi^2} + \frac{\partial \overline{v}}{\partial \xi} - \varphi - r^2 s^2 \lambda^3 (\lambda + \zeta) \frac{\partial^2 \varphi}{\partial \tau^2} - r^2 s^2 \lambda^3 \zeta \frac{\partial \varphi}{\partial \tau} = 0 ,$$

(1b)

where $\overline{v} \equiv v / L$ is the dimensionless total deflection, φ represents the rotation of the beam cross section, $\xi \equiv x / L$ is a

dimensionless spatial coordinate, and $\tau \equiv \omega t$ is dimensionless time. The "Timoshenko beam parameters," *r* and *s*, are defined as the rotational inertia parameter and the shear deformation parameter, respectively, via [12, 13]

$$r^2 \equiv \frac{I}{AL^2} = \frac{1}{12}\left(\frac{b}{L}\right)^2 \quad , \quad s^2 \equiv \frac{EI}{kAGL^2} = \frac{1}{12}\left(\frac{b}{L}\right)^2\left(\frac{E}{kG}\right) \quad ,$$

(2a, b)

where $A=bh$, $I= hb^3/12$, and $k=5/6$ is the shear coefficient for a rectangular cross section. The dimensionless frequency and fluid resistance parameters, λ and ζ , are related to the fundamental system parameters by

$$\lambda \equiv \left(\frac{12\rho_b L^4 \omega^2}{Eb^2}\right)^{1/4} \quad , \quad \zeta \equiv \frac{L}{hb^{1/2}}\left(\frac{48\rho_f^2 \eta^2}{E\rho_b^3}\right)^{1/4} \, .$$

(3a, b)

The governing equations are accompanied by four boundary conditions (BCs). For Load Case I, the BCs are

$$\overline{v}(0,\tau) = 0 \quad , \quad \varphi(0,\tau) = \theta_o e^{i\tau} \quad , \quad \frac{\partial\varphi(1,\tau)}{\partial\xi} = 0 \quad , \quad \frac{\partial\overline{v}(1,\tau)}{\partial\xi} - \varphi(1,\tau) = 0 \quad ,$$

(4a-d)

while for Load Case II the following BCs apply:

$$\overline{v}(0,\tau) = 0 \quad , \quad \varphi(0,\tau) = 0 \quad , \quad \frac{\partial\varphi(1,\tau)}{\partial\xi} = 0 \quad , \quad \frac{\partial\overline{v}(1,\tau)}{\partial\xi} - \varphi(1,\tau) = s^2\overline{F}_0 e^{i\tau} \, ;$$

(5a-d)

where

$$\overline{F}_0 \equiv F_0 L^2 / EI \, .$$

(6)

The boundary value problems (BVPs) to be solved consist of the governing equations, Eqs. (1a,b), and the corresponding set of BCs: Eqs. (4a-d) for Load Case I (harmonic support rotation) and Eqs. (5a-d) for Load Case II (harmonic tip force). These BVPs may be solved in analytical form, the details of which will not be presented here, but may be found in Ref. 14. Once the solution for the beam response

($\bar{v}$ and φ) is obtained, any other field of interest may be derived. In particular, the beam displacement due to bending deformation, $v_{B\text{-}D}$, may be expressed in normalized form as

$$\overline{v}_{B-D}(\xi,\tau) \equiv \frac{v_{B-D}(\xi,\tau)}{L} = \begin{cases} \displaystyle\int_0^{\xi} \varphi(\xi',\tau)d\xi' - \theta_0 \xi e^{i\tau} & , \text{ Load Case I;} \\[2em] \displaystyle\int_0^{\xi} \varphi(\xi',\tau)d\xi' & , \text{ Load Case II.} \end{cases}$$

(7a, b)

Note that the final term in Eq. (7a) is associated with removing the rigid-body rotation (see Fig. 2a) so that the result corresponds to the "bending-deformation displacement" that is associated only with bending strains that are being induced. The normalized shear displacement may be obtained for either load case by subtracting the bending displacement (including any rigid-body rotation) from the total displacement:

$$\overline{v}_S(\xi,\tau) \equiv \frac{v_S(\xi,\tau)}{L} = \overline{v}(\xi,\tau) - \int_0^{\xi} \varphi(\xi',\tau)d\xi' .$$

(8)

THEORETICAL RESULTS AND DISCUSSION

Frequency Spectra

The theoretical model may be used to generate frequency spectra, i.e., plots of the magnitude of the tip displacement amplitude versus the driving frequency for any output signal and for either load case (harmonic support rotation or tip force). In what follows the dynamic response of the beam will be characterized by three different output signals: D_T, $D_{B\text{-}D}$, and D_S, corresponding respectively to normalized values of total displacement at the beam tip (D_T) and the components of the tip displacement associated only with bending deformation ($D_{B\text{-}D}$) or shear deformation (D_S). Of primary interest are the resonant characteristics and not the entire frequency spectrum; however, for illustrative purposes we show some examples of frequency spectra in Figs. 3a and 3b for Load Cases I and II,

respectively. These figures correspond to fixed values of $r=0.2$ and $\zeta =1$ while the value of the material parameter

$$e \equiv \sqrt{E/kG} \tag{9}$$

is allowed to vary. Note that e corresponds to the relative size of the Young's modulus to the shear modulus and thus larger values of e correspond to the material having an increased susceptibility to shear deformation (i.e., smaller values of the shear modulus G). Since parameter e is independent of beam dimensions, we shall use it as a shear deformation parameter in place of parameter s (= er) defined in Eq. (2b).

The plots of Figs. 3a,b indicate that an increase in e results in a decrease in the resonant frequency as would be detected by any of the signals, which is to be expected due to the increasing flexibility of the model for larger e values. For the case of harmonic support rotation (Fig. 3a) an increase in e causes a decrease in the resonant amplitude of the total tip displacement (D_T), while for the harmonic tip force case (Fig. 3b) the resonant amplitude increases with increasing e. However, if one
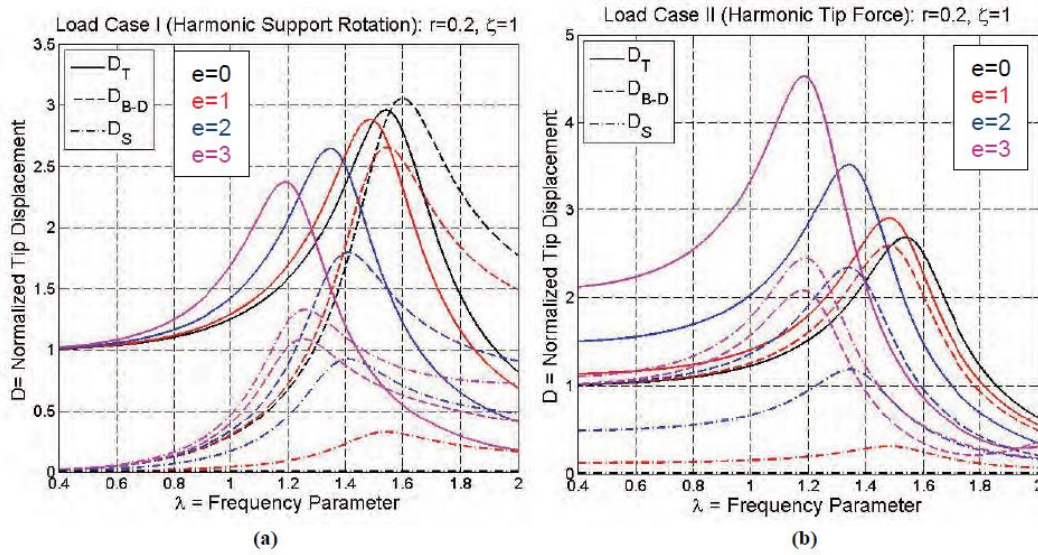

Fig. 3 Frequency Spectra for a Microcantilever Beam Vibrating Laterally in a Viscous Fluid for the Case $r = 0.2$, $\zeta = 1.0$, and $e = 0$ (black), 1 (red), 2 (blue), 3 (magenta) as Detected By Total, Bending-Deformation, and Shear Displacement at the Tip: (a) Load Case I; (b) Load Case II

considers the resonant amplitudes of the bending-deformation and shear portions of the tip displacement (D_{B-D} and D_S) as the value of e increases, one finds that the strength of the D_{B-D} signal at resonance decreases for both load cases, while the strength of the shear signal increases, as expected. Similar conclusions apply with respect to changes in the value of r, although the corresponding figures are not included here. For Load Case I it is interesting to note that the bendingdeformation displacement signal yields a larger resonant amplitude than the total displacement signal. This is associated with "misalignment" of the resonant peaks of the three output signals in Fig. 3a, which is due to the fact that the total displacement becomes more out-of-phase with the bending-deformation and shear displacements (and the imposed support rotation) as ζ increases. The different resonant amplitudes of the various output signals could have important implications with regard to the appropriate design of detection schemes for these types of sensing devices. For example, a detection scheme based on monitoring of bending strain (e.g., via piezoresistors at the extreme fibers of the beam near the support) might only "see" a small portion of the deformation response if a significant amount of shear deformation is present. In such a case, one may wish to replace or supplement the bending-strain detection scheme with shear strain measurements near the neutral axis of the beam's cross section.

The numerical results to follow in the remaining sections of the paper will focus on the resonant frequency and quality factor of lateral-mode mirocantilevers in liquids. Theoretical values of these resonant quantities may easily be extracted from frequency response curves of the type shown in Figs. 3a,b. For microscale devices in liquids whose properties are on the same order as that of water, the fluid resistance parameter lies in the range $0 \leq \zeta \leq 0.2$, in which case the values of resonant frequency and quality factor are very insensitive to both the load case and the output signal employed. However, for other applications (either at the nanoscale or in fluids with higher viscosity and/or density) the fluid resistance parameter may be much larger. In these cases there may be noticeable differences in resonant characteristics of the output signals generated by the different loading/detection schemes, as is apparent in Figs. 3a,b for the case of $\zeta = 1$. In the results that follow such differences between the total

and bending-deformation signals will be explored, but only Load Case I (harmonic support rotation) will be considered as it corresponds to the most common actuation method (electrothermal) used to date for lateralmode microcantilevers. (Similar results may easily be generated for the tip force case.)

Resonant Frequency

The resonant frequency parameter, λ_{res}, for the first lateral mode is plotted in Fig. 4 for the case of harmonic support rotation. The figure shows the dependence of resonant frequency on the Timoshenko parameters, as characterized by the geometric parameter r and material parameter e. These resonant frequency values correspond to the first peaks of the frequency spectra for the total displacement and the bending-deformation displacement at the tip (curves of the type plotted in Fig. 3a). The ranges of parameters considered in Fig. 4 include practical values of microcantilever dimensions and material properties expected to be encountered in lateral-mode MEMS sensing applications, including those necessitating the incorporation of shear deformation and rotatory inertia effects (i.e., when b/L is *not* small relative to unity).

Figure 4 clearly illustrates several trends. First, there is an expected reduction in resonant frequency associated with an increase in the fluid resistance parameter. This may be interpreted as follows: for fixed cantilever dimensions the resonant frequency will decrease if the fluid density or viscosity is increased. Also observed in Fig. 4 is how higher levels of Timoshenko parameters – larger r and e values, corresponding to increased rotational inertia and decreased shear stiffness of the beam – will result in a reduction in resonant frequency. Over the range of Timoshenko and fluid parameters considered in Fig. 4, the maximum effect of r and e is to cause a reduction of 26% in λ_{res} which, according to Eq. (8a), is equivalent to a decrease in the resonant frequency, ω_{res}, of 46%. These reductions correspond to the *DT* signal for the case of r=0.2, e=3 in Fig. 4b. If we consider the case e=2, which corresponds to "textbook" values of moduli for silicon in the frame of reference of a standard (100) silicon wafer [15], i.e., E=169 GPa, G=50.9 GPa, and a shear coefficient of k=5/6, Fig. 4b shows that the largest influence of the Timoshenko effects on the resonant frequency is a 17% decrease in λ_{res} (31% reduction in ωres),

which occurs at $r=0.2$. Clearly, significant error may be introduced in the resonant frequency estimate if the Timoshenko effects are ignored in such cases. Finally, as a verification of the resonant frequency results, we find that the value in Fig. 4a for the case $r = \zeta = 0$ (i.e., the starting value of the upper curve) is given by $\lambda_{res} = 1.8751$, which agrees with the well-known eigenvalue for an Euler-Bernoulli beam in vacuum [16].

The effect of a larger value of fluid resistance parameter (associated with smaller beam dimensions and/or increased values of fluid properties) may be seen by comparing the curves in Fig. 4a (small ζ) to those in Fig. 4b (larger ζ). In particular we note that the sensitivity of the resonant frequency to the output signal is negligible in the former case but becomes much more pronounced in the latter case of $\zeta = 1$. We observe that for cases of larger values of fluid resistance parameter, monitoring the bending deformation of the beam actually results in a noticeably higher resonant frequency than if one tracks the total tip displacement. This result is related to the previously mentioned fact that the total displacement becomes more out-of-phase with the bending-deformation and shear displacements as ζ increases, and may have important implications in sensor applications as the mass sensitivity tends to be higher at larger values of resonant frequency.
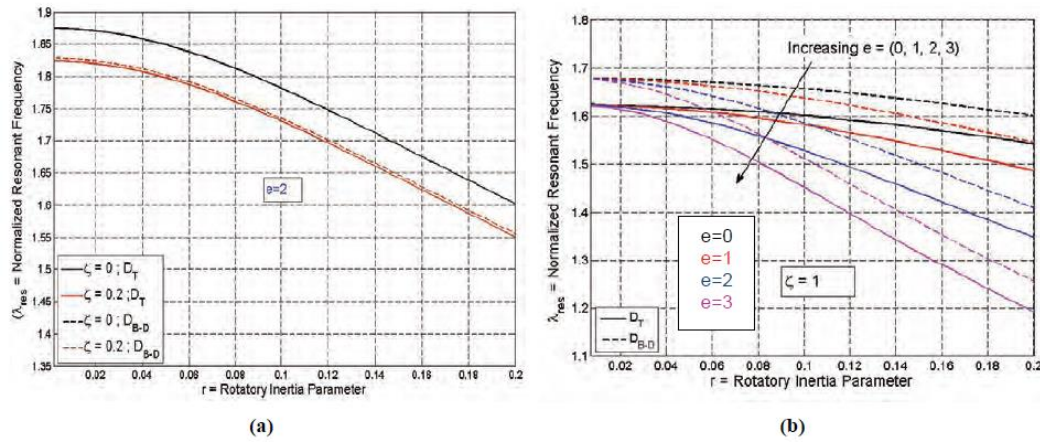

Fig. 4 Theoretical Values of Normalized Resonant Frequency of a Microcantilever Vibrating Laterally in a Viscous Fluid as Detected by Total and Bending-Deformation Tip Displacements for Load Case I: (a) Small Fluid Resistance Results ($\zeta = 0$ and $\zeta =0.2$); (b) Large Fluid Resistance Results ($\zeta = 1.0$)

Quality Factor

Applying the half-power (bandwidth) method to the theoretical frequency spectra such as those shown in Fig. 3, one may obtain the quality factor for a range of fluid resistance and Timoshenko parameters. For example, the quality factor based on both the total tip displacement and the bending-deformation portion are plotted in Fig. 5 for the case of harmonic support rotation loading over the range $\zeta \in [0, 1]$. The figure is based on specified values of r=0.2 (i.e., b/L=0.7) and e=2 (e.g., silicon). Clearly, there is a very strong impact of the fluid resistance parameter on the quality factor, with Q following what appears to be roughly an inverse relationship with ζ as was shown to be the case for a Bernoulli-Euler beam [3, 4]. Recalling the definition of ζ , the viscosity and density of the fluid participate to an equal extent in determining Q. Also apparent from Fig. 5 are the virtually identical results for Q as detected by the two types of output signals when ζ is small ($\zeta \leq 0.2$). However, at larger values of fluid resistance, the figure indicates a noticeable difference in the detected values of Q, with *DT* yielding a quality factor that is 11% higher than that based on the *DB-D* signal at $\zeta = 1$.

Unlike the strong dependence of Q on ζ , the effect of increasing the Timoshenko parameter e from 0 to 3 (not shown here) results in a relatively modest 15% reduction of the quality factor compared to the Bernoulli-Euler (e= 0) case, even for a relatively large value of r such as r=0.2 . Similarly, for a specified value of e between 0 and 3, changing r over the range 0 to 0.2 results in a modest reduction in Q that is no larger than 15%. Thus, based on the observations here and in the previous section, the model indicates that the Timoshenko effects have a stronger impact on the resonant frequency than on the quality factor.
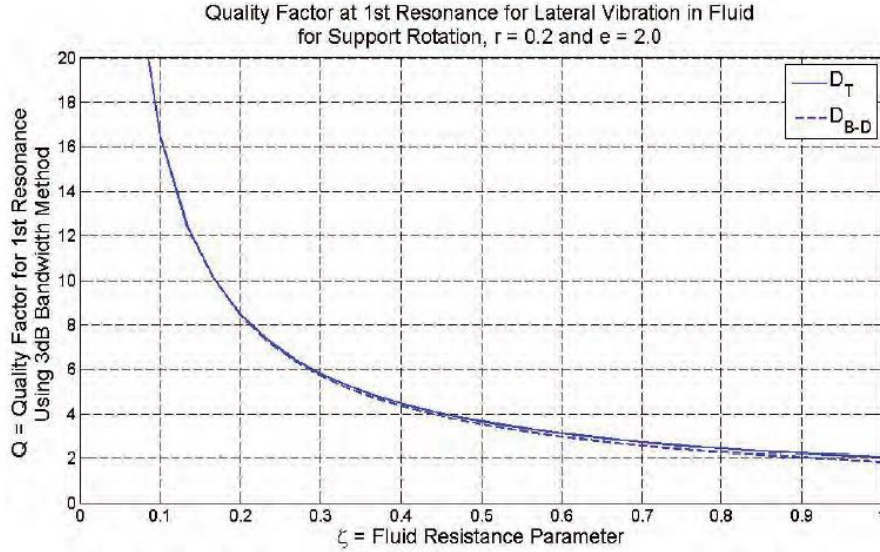
Fig. 5 Theoretical Quality Factor Based on Half-Power (Bandwidth) Method at First Resonance for Fluid Resistance Values $\zeta \in [0, 1]$ and Timoshenko Parameters $r = 0.2$ and $e = 2$ as Detected by *DT* and *DB-D*

COMPARISONS WITH EXPERIMENTAL DATA

In an attempt to validate the current model, the theoretical results were compared with experimental data for resonant frequency and quality factor for laterally excited microcantilevers in water. The beams were actuated electrothermally in a manner that may be modeled kinematically as an imposed support rotation as noted earlier. Details regarding device fabrication [5] and the testing procedure [7] are described elsewhere. Specimen geometries were grouped according to the nominal thicknesses of the Si substrate material, *hnom* = (5, 8, 12, 20) μm, and within each thickness set the length and width dimensions were as follows: L = (200, 400, 600, 800, 1000) μm, b = (45, 60, 75, 90) μm. For all of the theoretical calculations, estimates of the total thickness (Si plus several passivation layers) were used in lieu of the nominal silicon thicknesses. To generate theoretical results it was necessary to also specify numerical values of the following material parameters: $C1 \equiv \sqrt{E/12\rho_b}$ and $C2 \equiv e = \sqrt{E/kG}$. Due to the composite nature of the fabricated cantilevers (Si substrate plus several passivation layers), it is difficult to prescribe specific values of the effective Young's modulus E or shear modulus G *a priori.* Therefore, the values of the *C*1 parameter (for each thickness set)

were determined by fitting the *in-vacuum* results of the present model to *in-air* experimental frequency data (assuming that the air resistance has a negligible impact on the f_{res}). The *same* values of $C1$ were then used in making the comparison between the *in-water* results of the present model and the *in-water* experimental data, which is the comparison of main interest in this study. A similar approach may have been utilized to obtain best-fit $C2$ values by fitting the in-air frequency data; however, this would possibly result in "overfitting" the model to the data. To avoid this situation and thereby provide a more objective means of validating the model, the previously mentioned "textbook" value of $C2=2$ was used, as this corresponds to the orientation of the Si microbeams used. Note that the $C1$ value is associated with the initial slope of the resonant frequency vs. b/L^2 curves, while the $C2$ value corresponds to the degree of curvature of these curves (i.e., departure from linearity) at larger values of b/L^2. In all calculations for the in-water case, the fluid properties were specified as ρ_f = 1000 kg/m3 and η = 0.001 Pa·s in the model.

A sample of the theory vs. experimental data comparisons is shown in Fig. 6 for the resonant frequency for the first lateral mode. Only the comparison for the nominal thickness of 5 μm is included here (total thickness = 7.02 μm when passivation layers are included), but similar trends apply to the other thicknesses [14]. The comparison of resonant frequencies in Fig. 6 indicates that the model is able to simulate qualitatively the softening trend of the experimental data for the shorter, wider beams (larger b/L^2 values) for which the Timoshenko beam effects (shear deformation and rotatory inertia) are expected to be more pronounced. However, from a quantitative perspective the model underestimates the departure from the linear Bernoulli-Euler results, indicating that (a) the actual value of $C2$ is much larger than the specified value of 2, possibly due to the composite nature of the microstructure or imperfect bonding between layers, and/or (b) an additional softening effect is being neglected in the present model. With regard to the latter possibility, the most likely candidate would be the finite support compliance that is ignored in the present model which assumes a rigid support. As the beam becomes shorter and wider, not only do the Timoshenko beam effects become more important, but the flexural stiffness of the beam becomes relatively large in comparison with the rotational stiffness of the

support. As a result, there is a greater likelihood that the support will elastically deform during the vibration and that this will introduce an additional softening effect leading to even lower resonant frequencies such as those indicated by the data in Fig. 6. (This effect is currently being incorporated into the present Timoshenko beam model via an appropriate modification of the boundary conditions.)
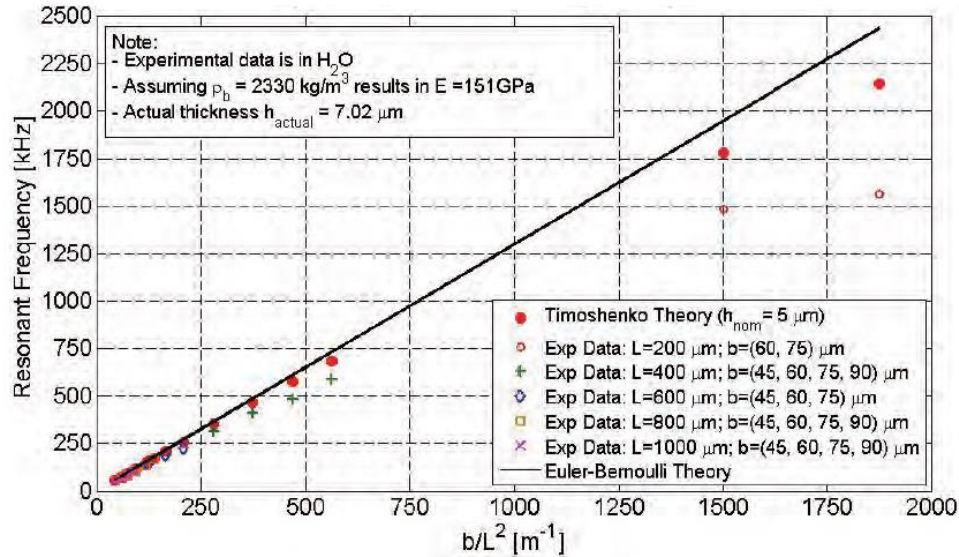

Fig. 6 Comparison of Current In-Fluid, Timoshenko Model to Experimental Resonant Frequency for First Lateral Flexural Mode, Nominal Thickness 5 μm Using $C1 = 2.3240$ km/sec and $C2 = 2$
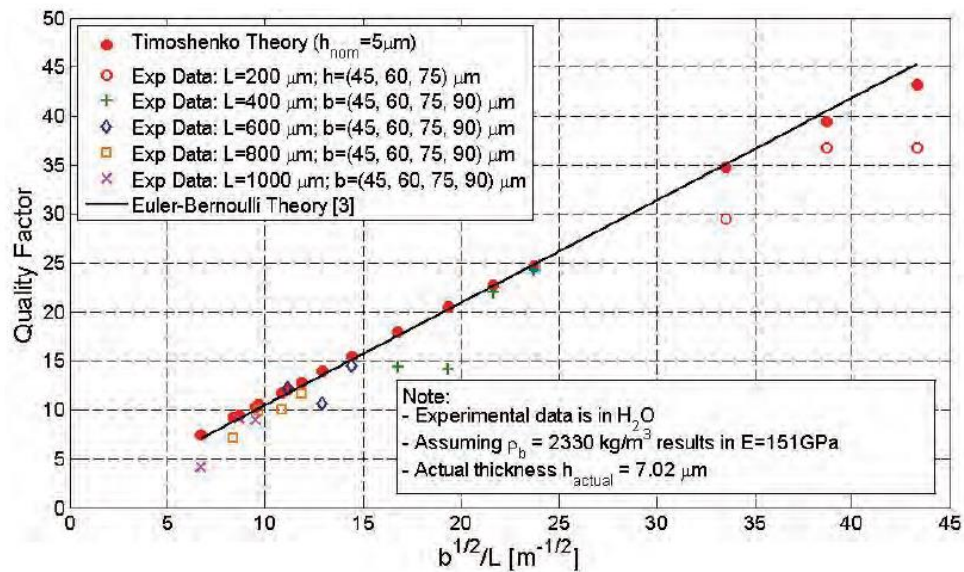
16

Fig. 7 Comparison of Current In-Fluid, Timoshenko Model to Experimental [7] Quality Factor for First Lateral Flexural Mode, Nominal Thickness 5 μm Using $C1 = 2.3240$ km/sec and $C2 = 2$

In Fig. 7 the comparison of theoretical results vs. experimental data is shown for the quality factor at the first resonance peak. Again, the comparison is shown only for the 5-μm nominal thickness specimens, but similar trends apply to the other thicknesses [14]. As was the case in the frequency comparison, the model is able to simulate qualitatively the softening trend of the experimental Q data for the shorter, wider beams (larger $b^{1/2}/L$ values) due to higher levels of shear deformation and rotatory inertia, but quantitatively the predicted Q values still remain larger than the experimental values. Possible reasons for this include those that were previously noted for the frequency comparison. Fig. 7 also indicates that the theoretical results for Q slightly overestimate the data even for the more slender specimens, indicating that the Stokes fluid resistance model is slightly underestimating the fluid damping and thereby giving a reasonable upper-bound estimate of the actual quality factor. As expected, the assumption of Stokes resistance yields reasonable estimates of Q for the thinner beams (in this case those with nominal thicknesses of 5 and 8 μm), but leads to a significant overestimation of Q for the thicker specimens (nominal thicknesses of 12 and 20 μm). We note that the departure of the experimental Q data from the linearity implied by Bernoulli-Euler theory is not as strong as that associated with the resonant frequency (compare Figs. 6 and 7), and the theoretical model shows a similar trend in this respect.

SUMMARY AND CONCLUSIONS

An analytical Timoshenko beam model that incorporates fluid effects via a Stokes-type fluid resistance assumption has been presented. The theoretical results for resonant frequency and quality factor have been shown to depend on the loading type and detection scheme for higher values of the fluid resistance parameter. Notably, the quality factor obtained from the total tip displacement was found to be higher than that associated with monitoring the bending deformation response (analogous to measuring flexural strains near the support). Comparisons between the analytical results and experimental data indicated that the analytical model provides an

improvement over the Bernoulli-Euler theory and yields the same qualitative trends exhibited by the data. These comparisons indicate that the quantitative results of the model, which provide reasonable estimates to the data in many cases, may be further improved by incorporating support compliance effects into the Timoshenko beam model presented in the present work.

ACKNOWLEDGMENTS

REFERENCES

1. Sharos, L.B., Raman, A., Crittenden, S., and Reifenberger, R., "Enhanced mass sensing using torsional and lateral resonances in microcantilevers," *Applied Physics Letters*, Vol. 84, pp. 4638-4640 (2004).

2. Dufour, I., Josse, F., and Heinrich, S., "Theoretical analysis of strong-axis bending mode vibrations for resonant microcantilever (bio)chemical sensors in gas or liquid phase" *Journal of Microelectromechanical Systems*, Vol. 16, pp. 44-49 (2007).

3. Heinrich, S.M., Maharjan, R., Beardslee, L., Brand, O., Dufour, I., and Josse, F., "An analytical model for in-plane flexural vibrations of thin cantilever-based sensors in viscous fluids: applications to chemical sensing in liquids," *Proceedings, International Workshop on Nanomechanical Cantilever Sensors*, Banff, Canada, May 26-28, 2010, 2 pp. (2010).

4. Heinrich, S.M., Maharjan, R., Dufour, I., Josse, F., Beardslee, L.A., and Brand, O., "An analytical model of a thermally excited microcantilever vibrating laterally in a viscous fluid," *Proceedings, IEEE Sensors 2010 Conference*, Waikoloa, Hawaii, November 1-4, 2010, pp. 1399-1404 (2010).

5. Beardslee, L., Addous, A., Heinrich, S., Josse, F., Dufour, I., and Brand, O., "Thermal excitation and piezoresistive detection of cantilever in-plane resonance modes for sensing applications," *Journal of Microelectromechanical Systems*, Vol. 19, pp. 1015-1017 (2010).

6. Beardslee, L.A., Demirci, K.S., Luzinova, Y., Mizaikoff, B., Heinrich, S.M., Josse, F., and Brand, O., "Liquid-phase chemical sensing using lateral

mode resonant cantilevers," *Analytical Chemistry*, Vol. 82, pp. 7542-7549 (2010).

7. Beardslee, L.A., Josse, F., Heinrich, S.M., Dufour, I., and Brand, O., "Geometrical considerations for the design of liquid-phase biochemical sensors using a cantilever's fundamental in-plane mode," *Sensors and Actuators B*, Vol. 164, pp. 7-14 (2012).

8. Cox, R., Josse, F., Heinrich, S., Brand, O., and Dufour, I., "Characteristics of laterally vibrating resonant microcantilevers in viscous liquid media," *Journal of Applied Physics*, Vol. 111, 014907, 14 pp. (2012).

9. Dufour, I., Josse, F., Heinrich, S., Lucat, C., Ayela, C., Menil, F., and Brand, O., "Unconventional uses of microcantilevers as chemical sensors in gas and liquid media," *Sensors and Actuators B*, Vol. 170, pp. 115-121 (2012).

10. Cox, R., Josse, F., Wenzel, M., Heinrich, S.M., and Dufour, I., "A generalized model of resonant polymer-coated microcantilevers in viscous liquid media," *Analytical Chemistry*, Vol. 80, pp. 5760-5767 (2008).

11. Stokes, G., "On the effects of the internal friction of fluids on the motion of pendulums" *Transactions of the Cambridge Philosophical Society*, Vol. 9, pp. 8-106 (1851).

12. Timoshenko, S., and Young, D.H., *Vibration Problems in Engineering*, Third Edition, Van Nostrand (1955).

13. Huang, T.C., "The effect of rotatory inertia and of shear deformation on the frequency and normal mode equations of uniform beams with simple end conditions," *Journal of Applied Mechanics*, Vol. 28, pp. 579-584 (1961).

14. Schultz, J. "Lateral-mode vibration of microcantilever-based sensors in viscous fluids using Timoshenko beam theory," *Ph.D. Dissertation*, Marquette University (2012).

15. Hopcroft, M., Nix, W., and Kenny, T., "What is the Young's modulus of silicon?" *Journal of Microelectromechanical Systems*, Vol. 19, pp. 229-238 (2010).

16. Clough, R.W., and Penzien, J., *Dynamics of Structures*, Second Edition, McGraw-Hill (1993).

About the Authors

Joshua A. Schultz : Civil and Environmental Engineering, Marquette University Milwaukee, WI

Email: joshua.schultz@outlook.com